Pore properties of hierarchically porous carbon monoliths with high surface area obtained from bridged polysilsesquioxanes

AUTHOR(S):

Hasegawa, George; Kanamori, Kazuyoshi; Nakanishi, Kazuki

CITATION:

Hasegawa, George ...[et al]. Pore properties of hierarchically porous carbon monoliths with high surface area obtained from bridged polysilsesquioxanes. Microporous and Mesoporous Materials 2012, 155: 265-273

ISSUE DATE:

2012-06

URL:

http://hdl.handle.net/2433/154893

Pore Properties of Hierarchically Porous Carbon Monoliths with High Surface Area Obtained from Bridged Polysilsesquioxanes

George HASEGAWA, Kazuyoshi KANAMORI* and Kazuki NAKANISHI

Department of Chemistry, Graduate School of Science, Kyoto University, Kitashirakawa, Sakyo-ku, Kyoto 606-8502, Japan.

Corresponding author: Kazuyoshi KANAMORI, Dr. Eng.

Department of Chemistry, Graduate School of Science, Kyoto University, Kitashirakawa, Sakyo-ku, Kyoto 606-8502, Japan.

Tel/Fax: +81 75 753 7673, E-mail: kanamori@kuchem.kyoto-u.ac.jp

ABSTRACT

Hierarchically porous carbon monoliths with high specific surface area have been prepared via a nano-phase extraction technique from carbon/silica composites which had been prepared from arylene-bridged polysilsesquioxanes. The nano-sized silica phase developed in the composite has been removed to increase micropores, resulting in a similar effect to thermal activation of carbons. The resultant

carbons are expected to possess homogeneously distributed micropores. Here we report the changes of the pore characteristics through the synthesis process by the nitrogen adsorption-desorption method and mercury porosimetry. In particular, the growth of silica phase in carbon/silica composites at different temperatures has been characterized by the micropore analysis using the Horváth-Kawazoe method.

Keywords

Hierarchically porous material; Nano-phase extraction; Carbon monolith with high surface area; Carbon/silica composite

1. Introduction

Various porous structures with different size levels including micropores, mesopores, and macropores are tailored using the sacrificial templating method called as nanocasting in various materials from organics to inorganics [1-8]. A number of carbon materials with controlled pore properties have been reported utilizing inorganic hard templates, such as mesoporous silica and zeolite [9-13]. Whereas this approach allows fabrication of highly-ordered porous structures when a suitable template can be prepared, the synthesis process requires multiple steps and tends to be laborious. Recently, simpler pathways for tailoring porous structures, especially microporous structure, in carbon materials were reported, in which nano-scaled carbon/silica composites are fabricated by the calcination of silica- or siloxane-based organic-inorganic hybrid materials prepared via the sol-gel route [14,15]. One of the phases is removed by chemical or thermal treatment to obtain microporosity, which we term nano-phase extraction. Liu *et al.* [14] successfully prepared mesoporous polymer-silica and carbon-silica nanocomposites by polymerizing phenolic resin and silica in parallel in a controlled sol-gel process. The resultant nanocomposites can be converted to pure carbon or to pure silica by the post treatments (etching or pyrolysis). Pang *et al.* [15] used phenylene-bridged alkoxysilane to prepare mesoporous hybrid followed by carbonization to obtain carbon/silica nanocomposites. The nanocomposite can be

converted into micro- and mesoporous carbons after removing the silica phase. Although these techniques offer versatility in obtaining porous carbons, silicas or their composites, and enable to shorten the synthesis process, the synthesis condition of the composites should be strictly controlled particularly in the Liu's method. Therefore, there have been only a few reports about the preparation of carbon particles with ordered porous structures and high surface areas [14,15]. When carbon/silica composites in other material shapes such as monolith are successfully fabricated, the possible applications of porous materials based on carbon/silica compositions will be largely extended.

So far, porous carbon monoliths have been synthesized by two processes. One process employs activated carbon powders and shapes into monoliths by using binders [16,17] or hot-pressing [18-20]. This method for preparing carbon monoliths with a macroporous structure is simple but is difficult to finely tune the pore properties. From the viewpoint of the application to catalyst supports and electrochemical devices, the hierarchical pore structures are required in order to make all the micropores throughout the whole monolith accessible. Mesopores and macropores enable an efficient materials transport in the porous media and increase available surface area. Another process employs the activation of porous carbon monoliths, which are mainly prepared from porous polymer monoliths with controlled pores [21-25]. The heat-treatment of the carbons in a mildly oxidative atmosphere such as in an N_2/CO_2 mixed gas flow or a steam flow increases the number of micropores resulting in carbon monoliths with high specific surface area. By this method, carbon monoliths with not only large amount of micropores but also controlled meso- and/or macropores can be fabricated. The pore properties of the resultant carbon monoliths, however, include inhomogeneity between inside and outside of the monoliths because the degree of exposure to the oxidative gas is significantly different; the inner parts of the monoliths are less-activated than the outer parts. For effective applications such as to monolithic electrodes for supercapacitors, the activation of precursor monoliths should therefore be performed on sufficiently small-sized pieces like a thin plate in order to allow an even gas exposure and enhance the homogeneity of pores in the whole monoliths [22,25].

Recently, we have reported that hierarchically porous carbon monoliths with high surface area are successfully prepared from the porous carbon/silica composites which were obtained from biphenylene-bridged polysilsesquioxane monoliths [26]. Well-defined macropores were tailored with the polysilsesquioxane networks by utilizing sol–gel method accompanied by spinodal decomposition [27,28]. Besides, mesopores were also introduced by the hydrothermal treatment of the polysilsesquioxanes in a weakly basic condition, resulting in the hierarchically porous structure [26,28]. After the carbonization of the polysilsesquioxane monoliths, the enhancement of microporosity can be achieved by removing the nano-scaled silica phase from the resultant carbon/silica composites (nano-phase extraction). The resultant carbon monoliths are expected to possess homogeneous pore properties in the whole monoliths no matter how large and thick the carbon monoliths are. In this study, we have prepared carbon monoliths with high surface area from biphenylene- and phenylene-bridged polysilsesquioxane monoliths, and changes of pore properties in the materials through the synthesis process has been investigated by mercury porosimetry and nitrogen physisorption measurements. The sizes of the nano-scaled silica phase in the carbon/silica composites prepared from different precursors have also been discussed.

2. Experimental

2.1 Chemicals

The precursor alkoxysilanes, 4,4'-bis(triethoxysilyl)-1,1'-biphenyl (BTEBP) and 1,4-bis(triethoxysilyl)benzene (BTEB), were purchased from Sigma-Aldrich Co. (USA). The solvent, *N*,*N*-dimethylacetamide (DMAc) and *N*,*N*-dimethylformamide (DMF), and sodium hydroxide (NaOH) were purchased from Kishida Chemical Co., Ltd. (Japan). Aqueous solution of nitric acid (HNO_3) in 65 wt % and urea were purchased from Hayashi Pure Chemical Industry Ltd. (Japan). Pluronic F127 (PEO_{106}-PPO_{70}-PEO_{106}) was obtained from BASF Co. (Germany). All reagents were used as received and distilled water was used in all experiments.

2.2 Synthesis

The bridged polysilsesquioxane gels were synthesized according to the previous reports [28,29]. In the case of biphenylene-bridged gels, 1.5 g of Pluronic F127 was dissolved in 8 mL of DMAc, and 0.5 mL of 1 M HNO_3 aq. was added. After the complete mixing, 2 mL BTEBP was added to the obtained homogeneous solution, followed by stiring for 3 min at room temperature for hydrolysis. In the case of phenylene-bridged gels, 1.0 g of Pluronic F127 was dissolved in 8 mL of DMF, and 0.5 mL of 1 M HNO_3 aq. was added. After the complete mixing, 2 mL BTEB was added to the obtained homogeneous solution and the precursor sol was obtained. The following synthesis processes were the same in both systems. The resultant sol was then stood at 60 ºC for 24 h for gelation and aging. The wet gels thus obtained were washed with ethanol (EtOH) followed by the stepwise solvent exchange from EtOH to H_2O. The resultant wet gels were subsequently subjected to the solvent exchange to 2-propanol followed by slow evaporative-drying at 40 ºC resulting in the xerogels. Some of the wet gels were hydrothermally treated in 1 M urea aq. at 120 ºC or 200 ºC for 24 h before drying. After washing with H_2O, the samples were subjected to 2-propanol and dried at 40 ºC resulting in the hydrothermally treated xerogels. The obtained xerogels were subsequently heat-treated at 800−1200 ºC for 2 h with a heating rate of 4 ºC min^{-1} under an argon flow at 1.0 L min^{-1}. The resultant carbon/silica composites were immersed in 1 M NaOH aq. at 60 ºC for 12 h exchanging with fresh solvent three times to remove silica. The obtained carbon monoliths were washed with H_2O at 60 ºC for 4 h for three times followed by drying at 60 ºC. After washing with H_2O, some carbon monoliths were subjected to the solvent exchange to 2-propanol followed by supercritical drying using supercritical carbon dioxide at 80 ºC and 14.0 MPa in an autoclave (All-round Smart-operating Isostatic Pressing Chamber (ASIP), Mitsubishi Materials Corp., Japan).

The carbon/silica composites prepared from BTEBP are denoted as BP-CS-*x*-*y*, while the carbon samples prepared from BTEBP which were obtained after the removal of silica are denoted as BP-C-*x*-*y*. Here, *x* and *y* represents the hydrothermal-treatment temperature (in the case of the sample without hydrothermal treatment, *x* is described as “wo”) and the calcination temperature, respectively. The

carbon/silica composites and carbon monoliths prepared from BTEB are denoted as P-CS-*x*-*y* and P-C-*x*-*y*. When *y* is 300, BP-CS-*x*-300 and P-CS-*x*-300 represent the polysilsesquioxane monoliths, not carbon/silica composites, heat-treated at 300 ºC. In addition, the carbon monoliths which were subjected to supercritical drying are denoted as (sample code)-SCD, such as BP-C-200-1200-SCD.

2.3 Characterization

Observation of the microstructures of the fractured surfaces of the samples was conducted by scanning electron microscopy (SEM) (JSM-6060S, JEOL, Japan) and FE-SEM (JSM-6700F, JEOL, Japan). A mercury porosimeter (Pore Master 60-GT, Quantachrome Instruments, USA) was used to characterize the macropores and bulk densities of the samples. Nitrogen adsorption-desorption (BELSORP-mini II, Bel Japan Inc., Japan) was employed to characterize the meso- and micropores of the samples. Detailed features of micropores were investigated at the low relative pressure range using another nitrogen adsorption-desorption device (ASAP 2010, Micrometritics, USA) utilizing the Horváth-Kawazoe method.[30] Before nitrogen adsorption-desorption measurements, the samples were degassed at 300 ºC under vacuum for more than 6 h. Helium pycnometry (Accupyc 1330, Micromeritics, USA) was employed to determine true density of the samples. Porosity (%) of each sample was calculated as $(1-\rho_b/\rho_s) \times 100$, where ρ_b and ρ_s are bulk density and true density, respectively.

3. Results and Discussions

Figure 1 depicts the synthesis pathway of the samples. Porous carbon monoliths with high specific surface area have previously been obtained via carbon/silica composite, which were prepared from polysilsesquixane monolithic gels [26]. In this study, we have prepared the macroporous polysilsesquioxane precursor gels from two bridged-alkoxysilanes; biphenylene- and phenylene-bridged alkoxysilanes shown in Figure 2. As reported previously [28,29], both bridged-alkoxysilanes give rise to macroporous polysilsesquioxane monoliths via the sol–gel method accompanied by spinodal

decomposition. Besides, the hydrothermal treatment in the weakly basic aqueous solution tailors the mesoporosity with decreasing the amount of micropores by the Ostwald ripening as shown in Figure 3 [29]. After the hydrothermal treatment in the same condition, the phenylene-bridged polysilsesquioxane possessed the larger mesopores than the biphenylene-bridged one, which indicates that the polysilsesquioxane network with the larger organic groups shows the better resistivity against the alkaline solution. This is presumably because the biphenylene-bridged polysilsesquioxane is more hydrophobic than the phenylene-bridged one and less soluble in aqueous alkaline solution. In this study, we have used the polysilsesquioxane monoliths that have not undergone hydrothermal treatment (samples with micro- and macropores but without mesopores) as the precursors to investigate the changes in micropores. The polysilsesquioxane monoliths that have undergone hydrothermal treatment (samples with micro-, meso-, and macropores) were used as precursors for the investigation of the whole pore properties.

3.1 Biphenylene-bridged system

Since the crystallization of SiC takes place when the calcination temperature is more than 1300 ºC [26,28,29], the calcination temperatures were decided as 800 ºC, 1000 ºC, and 1200 ºC. Figure 4 a-c show the macroporous structure of the biphenylene-bridged polysilsesquioxane, the carbon/silica composite, and the carbon monolith, respectively. It is found that well-defined interconnected porous structure was obtained in all the samples. The resultant carbon material remained as the crack-free monolith even without supercritical drying as shown in Figure 4 d. The weight losses of the samples through the removal of silica were about 40 %.

The nitrogen physisorption isotherms of the carbon/silica composites and the carbon monoliths prepared with varied calcination temperatures are shown in Figure 5, and the pore characteristics of the samples are shown in Table 1. It indicates that only micropores increased and no mesopores were generated by the removal of silica. The increase in the micropores of BP-CS-wo-1000 was the largest among three BP-CS samples. The micropore size distributions of the samples calculated by the HK

method before and after the removal of silica are shown in Figure 6 a,c and b,d, respectively. From 800 ºC to 1000 ºC, the amount of micropores in the composite decreased in the micropore size range as shown in Figure 6 c because of the densification upon sintering. From 1000 ºC to 1200 ºC, the mean micropore size obviously shifted to the larger size, and the micropores of the width of 0.5−0.8 nm increased. This is because of the activation of the carbon phase [31], which increases micropores by making through-pores to isolated pores and enlarging the pore size. The activation usually takes place at above 800−950 ºC in the presence of an oxidative gas, such as CO_2 and H_2O [31,32]. In this case, a small amount of oxidative gases in argon gas as well as the oxygen involved in the carbon/silica composite enhances the activation. After the removal of silica, the micropores have dramatically increased as shown in Figure 5 and 6. The increase in micropores can be explained by two factors; one is the decrease in bulk density and the other is the removal of nano-phase silica. Since shrinkage both upon the removal of silica and upon the following drying may resist the increase in micropores, the shrinkage during drying after the removal of silica has been investigated with the supercritically-dried samples as shown in Figure S1. The isotherms suggest that only a little shrinkage took place during evaporative drying. Unfortunately, it was difficult to inquire the shrinkage during the removal of silica in the aqueous basic solution. Comparing Figure 6 a and b, it is found that micropores less than 1.5 nm increased in number. Since no mesopores were generated by removing silica, it is deduced that nano-sized silica (~1.5 nm) had been dispersed in the carbon/silica composites. Although the micro- and mesopore volumes were almost the same between BP-C-wo-1000 and BP-C-wo-1200, the specific surface area of BP-C-wo-1000 was higher than BP-C-wo-1200 as shown in Table 1, due to the smaller micropore size in BP-C-wo-1000 as shown in Figure 6 d.

The effect of the calcination temperature on the change of mesopores was investigated using the samples prepared with the hydrothermal treatment as shown in Figure 7. The mesopores retained after the calcination in all the carbon/silica composites. However, the mesopores retained after the removal of silica only when the sample was calcined at 1200 ºC. The carbonization at higher temperature enhanced the mechanical rigidity of the carbon part in the carbon/silica composites, which suppressed

the shrinkage and kept the mesoporosity after the removal of silica. The mean mesopore diameter of BP-C-200-1200 was calculated as 4.9 nm by the Barret-Joyner-Halenda (BJH) method. The difference of mesopore region between the carbon monoliths without and with mesopores was observed by FE-SEM as shown in Figure 8. The carbon monolith without mesopores was composed of the densely-packed smaller particles compared to that with mesopores. The interstices of the particles with a diameter of several tens nanometers were detected as mesopores in BP-C-200-1200.

3.2 Phenylene-bridged system

When the phenylene-bridged polysilsesquioxanes were used as the precursor, the well-defined macroporous structure has retained both after the calcination and removal of silica like the biphenylene-bridged system as shown in Figure 9. We have already investigated the effect of the calcination temperature and found that the mesopores were obtained only when the calcination temperature is 1200 ºC. In the phenylene-bridged system, the calcination temperature was therefore fixed at 1200 ºC. The change of the micro- and mesopore characteristics is summarized in Figure 10 and Table 2. It is found that P-CS-wo-1200 possesses only a few micropores whereas P-CS-200-1200 possesses the larger amount of micropores. In the biphenylene-bridged system, the carbon/silica composites prepared without hydrothermal treatment retained the microporosity (Figure 5). This difference is derived from the different organic bridging groups. The phenylene-bridged polysilsesquioxane without hydrothermal treatment largely shrinks during heat treatment, resulting in the collapse of micropores. On the other hand, the bulky biphenylene groups may enhance the rigidity of the polysilsesquioxane network, which suppresses the large shrinkage as well as the reduction of micropores. Also, the carbon/silica ratio of phenylene-bridged samples is smaller than that of biphenylene-bridged ones (the weight loss on the removal of silica were about 65 % for P-CS samples, compared to 40 % for BP-CS samples), which enhances the shrinkage during drying in P-CS samples. For the P-CS-200-1200 sample prepared with the hydrothermal treatment, the mesopores as well as micropores retained after the calcination in contrast to P-CS-wo-1200 due to the higher siloxane crosslinking density. The subsequent removal of

silica increased the amount of micropores in P-C-200-1200, while the mesopores are collapsed in contrast to BP-C samples shown in Figure 7. Supercritical drying allows the resultant carbon monoliths to retain well-defined mesopores as well as micropores. In particular, the micro-, meso- and macroporous hierarchical structure is obtained in P-C-200-1200-SCD. The mean mesopore diameter of the sample was calculated as 10.7 nm by the BJH method. The FE-SEM observation of P-C-200-1200 and P-C-200-1200-SCD were performed as shown in Figure 11. The cross section of the skeleton of P-C-200-1200 is relatively smooth. On the other hand, in P-C-200-1200-SCD, the interstices of the particles can be clearly observed, which correspond to the mesopores. This result agrees with the nitrogen physisorption results shown in Figure 10 b.

The changes of micropores in the samples calcined at 1200 ºC by removing silica are shown in Figure 12. In general, the micropore size of P-C-wo-1200 is obviously smaller than that of P-C-wo-1200-SCD due to the shrinkage during drying as described above. The increase in micropores larger than 1.5 nm is more significant in the phenylene-bridged system than the biphenylene-bridged system. In addition, the mesopore volume of P-C-wo-1200 is larger than that of BP-C-wo-1200. This result indicates that the size of the silica phase in P-CS-wo-1200 was larger than that in BP-CS-wo-1200. This is because of the enhanced growth of silica phase during calcination in the phenylene-bridged polysilsesquioxanes due to the larger silica content.

3.3 Change of macropore characteristics

The macropore properties and the porosities of the samples prepared with the hydrothermal treatment were summarized in Figure 13 and Table 3, respectively. The skeletal densities decreased after the removal of silica due to the lower density of carbon than silica. In both cases, the narrow macropore size distributions can be observed in all the samples. As discussed above, in the case of the phenylene-bridged samples, the larger shrinkage during drying after the removal of silica caused the larger decrease in porosity. The supercritical drying inhibited the shrinkage leading to the higher porosity and the larger macropore volume in P-C-200-1200-SCD. On the other hand, in the case of the samples

prepared from biphenylene-bridged polysilsesquioxanes, the relatively small shrinkage during drying resulted in the higher porosity (up to 90 %) of the carbon monoliths even without supercritical drying.

4. Conclusions

Hierarchically porous carbon monoliths with high specific surface area have been prepared by nano-phase extraction from the carbon/silica composites. The biphenylene- and phenylene-bridged polysilsesquioxane monoliths with well-defined macropores, which had been fabricated by the sol–gel method accompanied by phase separation, were calcined under inert atmosphere, resulting in the macroporous carbon/silica composites. The biphenylene-bridged polysilsesquioxanes yields relatively carbon-rich carbon/silica composites, whereas the phenylene-bridged polysilsesquioxanes yields silica-rich carbon/silica composites depending on the carbon contents of the precursor gels. The micropore analysis by the HK method revealed that the size of the silica grains in carbon/silica composites prepared from biphenylene-bridged polysilsesquioxanes was ~1.5 nm. In the case of phenylene-bridged ones, the size of silica grains was relatively larger because the enhanced growth of silica grains by sintering during the calcination.

The hierarchically porous carbon monoliths with specific surface area of > 1500 $m^2 g^{-1}$ can be obtained without supercritical drying when starting from biphenylene-bridged polysilsesquioxanes. Although the supercritical drying is necessary for retaining mesopores, the hierarchically porous carbon monoliths with relatively large mesopores (mean mesopores diameter was 10.7 nm) and specific surface area of > 1100 $m^2 g^{-1}$ can be prepared when phenylene-bridged polysilsesquioxane is chosen as the precursor. Since the micropores development by nano-phase extraction is advantageous in homogeneity compared to physical or chemical activation, extended applications of monolithic porous carbon materials such as to electrochemical devices, catalyst supports, and adsorbents are promising.

ACKNOWLEDGMENT

The present work was supported by the Grant-in-Aid for Scientific Research (No. 22·75 for G.H., No. 22750203 for K.K. and 20350094 for K.N.) from the Ministry of Education, Culture, Sports, Science and Technology (MEXT), Japan. Also acknowledged is the Global COE Program "International Center for Integrated Research and Advanced Education in Materials Science" (No. B-09) of the MEXT, Japan, administrated by the Japan Society for the Promotion of Science (JSPS).

Supporting Information Available.

Nitrogen adsorption-desorption isotherms of the evaporatively-dried and supercritically-dried carbon monoliths from biphenylene-bridged polysilsesquioxanes.

References

[1] P. Jiang, K.S. Hwang, D.M. Mitteleman, J.F. Bertone, V.L. Colvin, J. Am. Chem. Soc. 121 (1999) 11630-11637.

[2] A. Huczko, Appl. Phys. A 70 (2000) 365-376.

[3] K.H. Rhodes, S.A. Davis, F. Caruso, B. Zhang, S. Mann, Chem. Mater. 12 (2000) 2832-2834.

[4] J. Banhart, Prog. Mater. Sci. 46 (2001) 559-632.

[5] A. Stein, Micropor. Mesopor. Mater. 44 (2001) 227-239.

[6] J.M. Taboas, R.D. Maddox, P.H. Krebsbach, S.J. Hollister, Biomaterials 24 (2003) 181-194.

[7] A. H. Lu, F. Schüth, Adv. Mater. 18 (2006) 1793-1805.

[8] H. Nakajima, Prog. Mater. Sci. 52 (2007) 1091-1173.

[9] R. Ryoo, S.H. Joo, S. Jun, J. Phys. Chem. B 103 (1999) 7743-7746.

[10] H. Yang, D. Zhao, J. Mater. Chem. 15 (2005) 1217-1231.

[11] T. Kyotani, T. Nagai, S. Inoue, A. Tomita, Chem. Mater. 9 (1997) 609-615.

[12] J. Lee, J. Kim, T. Hyeon, Adv. Mater. 18 (2006) 2073-2094.

[13] A. Taguchi, J.H. Smått, M. Lindén, Adv. Mater. 15 (2003) 1209-1211.

[14] R. Liu, Y. Shi, Y. Wan, Y. Meng, F. Zhang, D. Gu, Z. Chen, B. Tu, D. Zhao, J. Am. Chem. Soc. 128 (2006) 11652-11662.

[15] J. Pang, V.T. John, D.A. Loy, Z. Yang, Y. Lu, Adv. Mater. 17 (2005) 704-707.

[16] K. Inomata, K. Kanazawa, Y. Urabe, H. Hosono, T. Araki, Carbon 40 (2002) 87-93.

[17] D. Lozano-Castelló, D. Cazorla-Amorós, A. Linares-Solano, D.F. Quinn, Carbon 40 (2002) 2817-2825.

[18] E. Bekyarova, K. Murata, M. Yudasaka, D. Kasuya, S. Iijima, H. Tanaka, H. Kahoh, K. Kaneko, J. Phys. Chem. B 107 (2003) 4681-4684.

[19] P.X. Hou, H. Orikasa, H. Itoi, H. Nishihara, T. Kyotani, Carbon 45 (2007) 2011-2016.

[20] J.M. Ramos- Fernández, M. Martínez-Escandell, F. Rodríguez-Reinoso, Carbon 46 (2008) 365-389.

[21] M. Lopez, M. Labady, J. Laine, Carbon 34 (1996) 825-827.

[22] R.W. Pekala, J.C. Farmer, C.T. Alviso, T.D. Tran, S.T. Mayer, J.M. Miller, B. Dunn, J. Non-Cryst. Solids 225 (1998) 74-80.

[23] A. Siyasukh, P. Maneeprom, S. Larpkiattaworn, N. Tonanon, W. Tanthapanichakoon, H. Tamon, T. Charinpanitkul, Carbon 46 (2008) 1309-1315.

[24] G. Hasegawa, K. Kanamori, K. Nakanishi, T. Hanada, Carbon 48 (2010) 1757-1766.

[25] G. Hasegawa, M. Aoki, K. Kanamori, K. Nakanishi, T. Hanada, K. Tadanaga, J. Mater. Chem. 21 (2011) 2060-2063.

[26] G. Hasegawa, K. Kanamori, K. Nakanishi, T. Hanada, Chem. Commun. 46 (2010) 8037-8039.

[27] K. Nakanishi, J. Porous Mater. 4 (1997) 67-112.

[28] G. Hasegawa, K. Kanamori, K. Nakanishi, T. Hanada, Chem. Mater. 22 (2010) 2541-2547.

[29] G. Hasegawa, K. Kanamori, K. Nakanishi, T. Hanada, J. Mater. Chem. 19 (2009) 7716-7720.

[30] G. Horváth, K. Kawazoe, J. Chem. Eng. Japan 16 (1983) 470-475.

[31] H. Jüntgen, Carbon 15 (1977) 273-283.

[32] F. Rodríguez-Reinoso, M. Molina-Sabio, M.T. González, Carbon 33 (1995) 15-23.

TABLES.

Table 1. Pore characteristics of the carbon/silica composites and the carbon monoliths based on biphenylene-bridged polysilsesquioxanes.

	S (α_s) [a] /m^2 g^{-1}	S (t-plot) [b] /m^2 g^{-1}	V_{micro} [c] /cm g^{-1}	V_{meso} [d] /cm g^{-1}
BP-CS-wo-800	670	640	0.209	0.030
BP-CS-wo-1000	430	440	0.161	0.034
BP-CS-wo-1200	830	780	0.191	0.066
BP-CS-200-1200	1000	1060	0.392	0.611
BP-C-wo-800	1610	1130	0.473	0.074
BP-C-wo-1000	2140	1870	0.560	0.082
BP-C-wo-1200	1630	1580	0.575	0.082
BP-C-200-1200	1420	1550	0.606	0.841

[a] specific surface area calculated by α_s method. [b] specific surface area calculated by t-plot method. [c] micropore volume calculated by the HK method. [d] mesopore volume calculated by BJH method.

Table 2. Difference in the pore characteristics of the evaporative-dried and supercritically dried carbon monoliths based on phenylene-bridged polysilsesquioxanes.

	S (α_s) [a] /m^2 g^{-1}	S (t-plot) [b] /m^2 g^{-1}	V_{micro} [c] /cm g^{-1}	V_{meso} [d] /cm g^{-1}
P-C-wo-1200	1380	1480	0.549	0.128
P-C-200-1200	930	1020	0.361	0.228
P-C-wo-1200-SCD	1630	1620	0.579	0.183
P-C-200-1200-SCD	1110	1170	0.480	1.143

[a] specific surface area calculated by α_s method. [b] specific surface area calculated by t-plot method. [c] micropore volume calculated by the HK method. [d] mesopore volume calculated by BJH method.

Table 3. Densities and porosities of the carbon/silica composites and the carbon monoliths.

	ρ_s [a] /g cm^{-3}	ρ_b [b] /g cm^{-3}	Porosity [c] /%
P-CS-200-1200	2.27	0.422	81
P-C-200-1200	1.83	0.432	76
P-C-200-1200-SCD	1.85	0.275	85
BP-CS-200-1200	2.48	0.314	87
BP-C-200-1200	2.13	0.215	90

[a] skeletal density measured by He pycnometry. [b] bulk density measured by Hg porosimetry. [c] calculated by $(1-\rho_b/\rho_s) \times 100$.

FIGURE CAPTIONS

Figure 1. Synthesis pathway of hierarchically porous carbon monoliths with high surface area.

Figure 2. Structural formula of the arylene-bridged alkoxysilanes used in this study.

Figure 3. Nitrogen adsorption-desorption isotherms of the bridged polysilsesquioxanes heat-treated at 300 °C with and without hydrothermal treatment; (a) biphenylene-bridged polysilsesquioxane and (b) phenylene-bridged polysilsesquioxane.

Figure 4. SEM images of (a) BP-CS-200-300, (b) BP-CS-200-1200, and (c) BP-C-200-1200. (d) Appearance of the resultant carbon monolith (BP-C-200-1200).

Figure 5. Nitrogen adsorption-desorption isotherms of the carbon/silica composites and the carbon monoliths based on biphenylene-bridged polysilsesquioxanes which were prepared without hydrothermal treatment and calcined at different temperatures. (b) is semi-logarithmic chart of (a).

Figure 6. Micropore size distributions of the carbon/silica composites (a,c) and the carbon monoliths (b,d) based on biphenylene-bridged polysilsesquioxanes which were prepared without hydrothermal treatment and calcined at different temperatures; (c) and (d) are the magnified chart of (a) and (b).

Figure 7. Nitrogen adsorption-desorption isotherms of the carbon/silica composites and the carbon monoliths based on biphenylene-bridged polysilsesquioxanes which were prepared with hydrothermal treatment and calcined at different temperatures.

Figure 8. FE-SEM images of the cross section of the sample skeleton; (a) BP-C-wo-1200 and (b) BP-C-200-1200.

Figure 9. SEM images of (a) P-CS-200-300, (b) P-CS-200-1200, (c) P-C-200-1200, and (d) P-C-200-1200-SCD.

Figure 10. Nitrogen adsorption-desorption isotherms of the samples based on phenylene-bridged polysilsesquioxanes; (a) samples without hydrothermal treatment and (b) samples with hydrothermal treatment.

Figure 11. FE-SEM images of the cross section of the sample skeleton; (a) P-C-200-1200 and (b) P-C-200-1200-SCD.

Figure 12. Micropore size distributions of the carbon/silica composites and the carbon monoliths calcined at 1200 ºC; (a) samples based on phenylene-bridged polysilsesquioxanes (inset is magnified chart) and (b) samples based on biphenylene-bridged polysilsesquioxanes.

Figure 13. Macropore size distributions of the carbon/silica composites and the carbon monoliths calcined at 1200 ºC; (a) samples based on phenylene-bridged polysilsesquioxanes and (b) samples based on biphenylene-bridged polysilsesquioxanes.

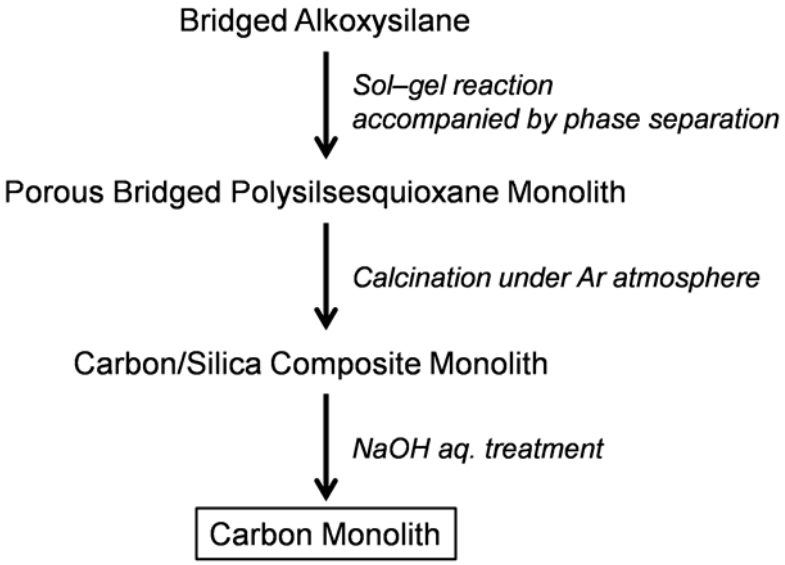

Figure 1

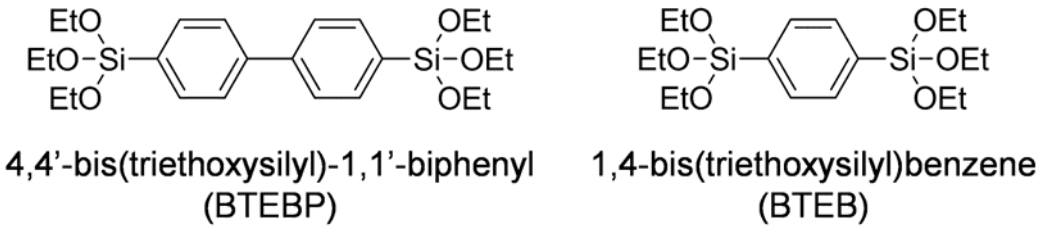

Figure 2

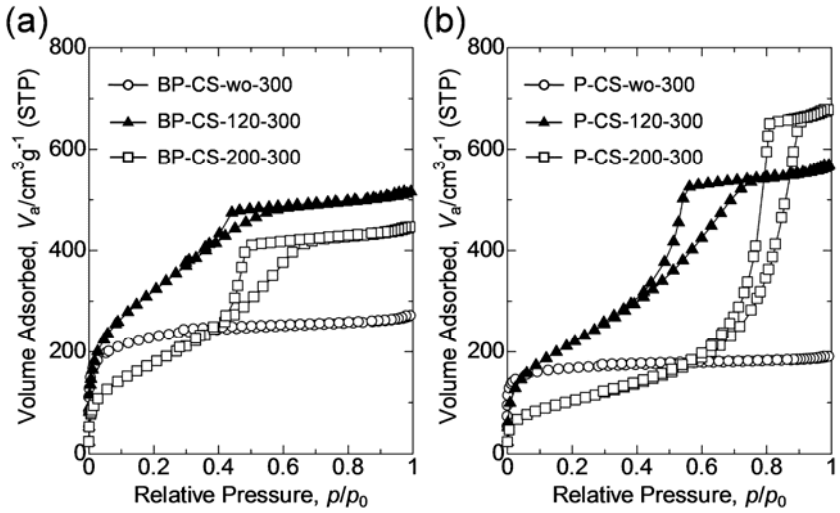

Figure 3

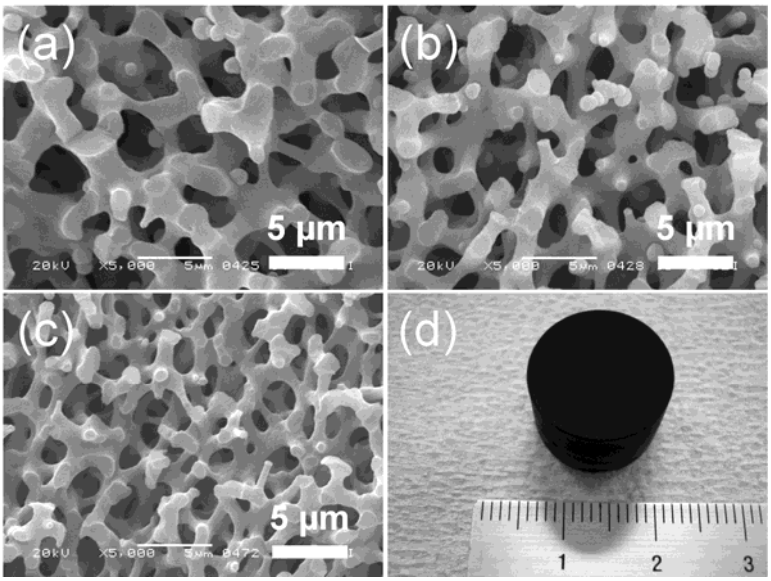

Figure 4

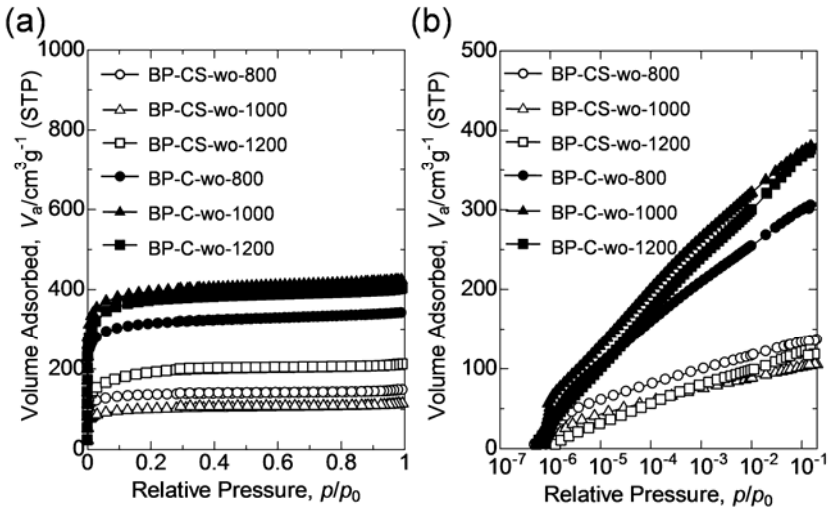

Figure 5

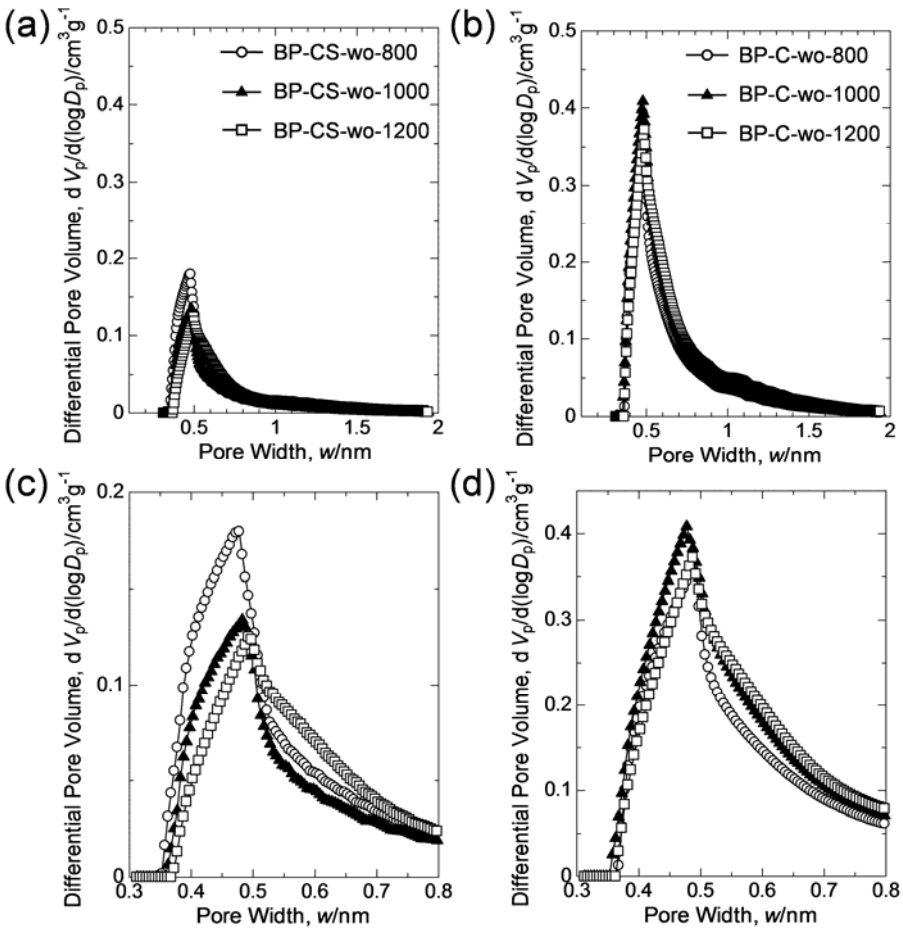

Figure 6

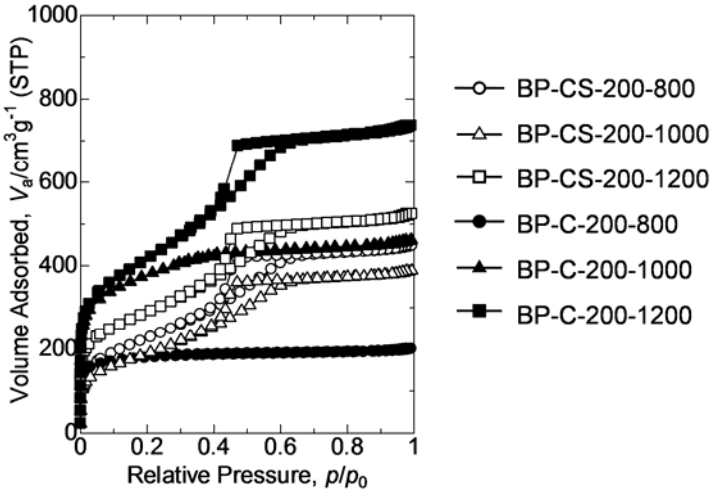

Figure 7

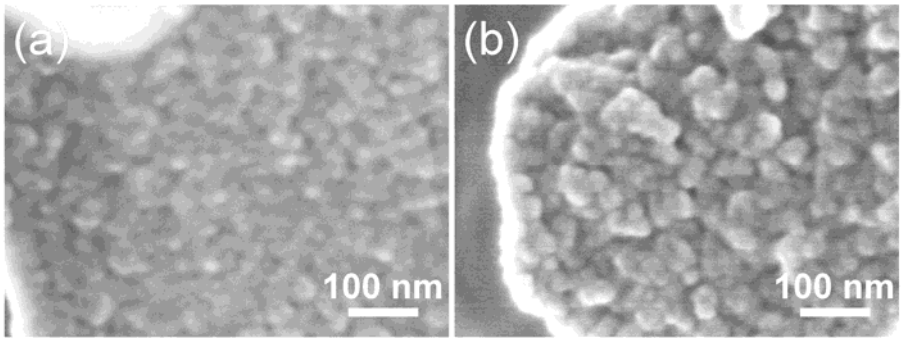

Figure 8

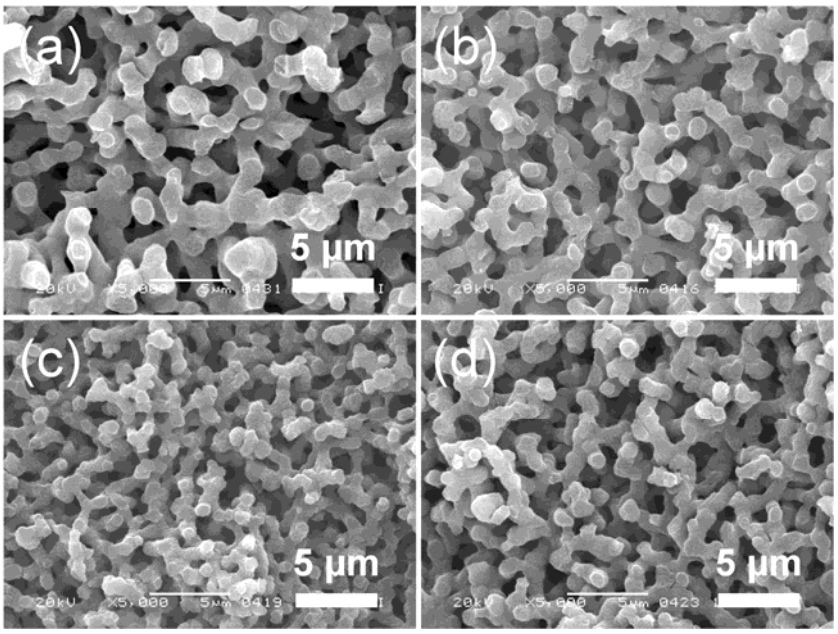

Figure 9

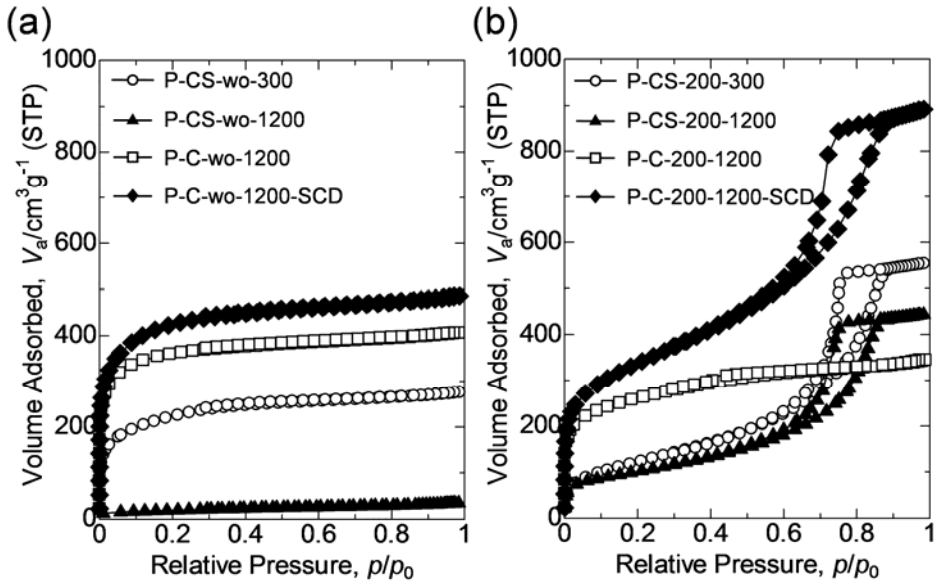

Figure 10

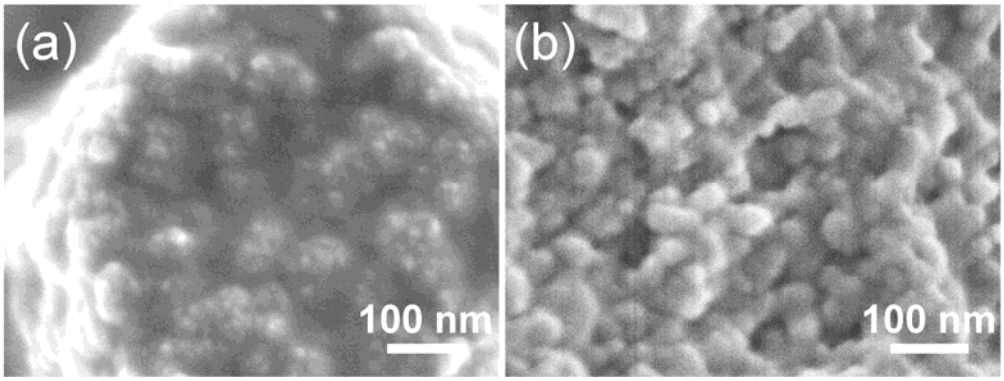

Figure 11

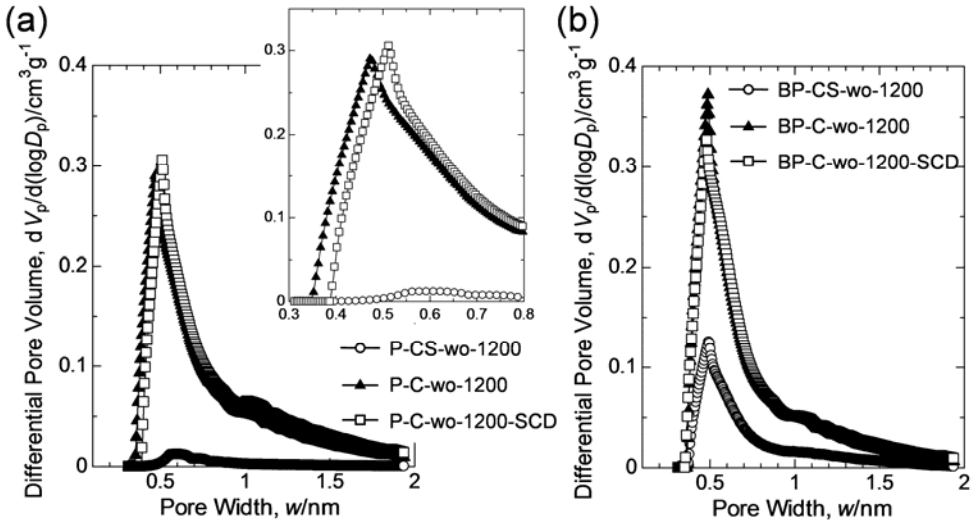

Figure 12

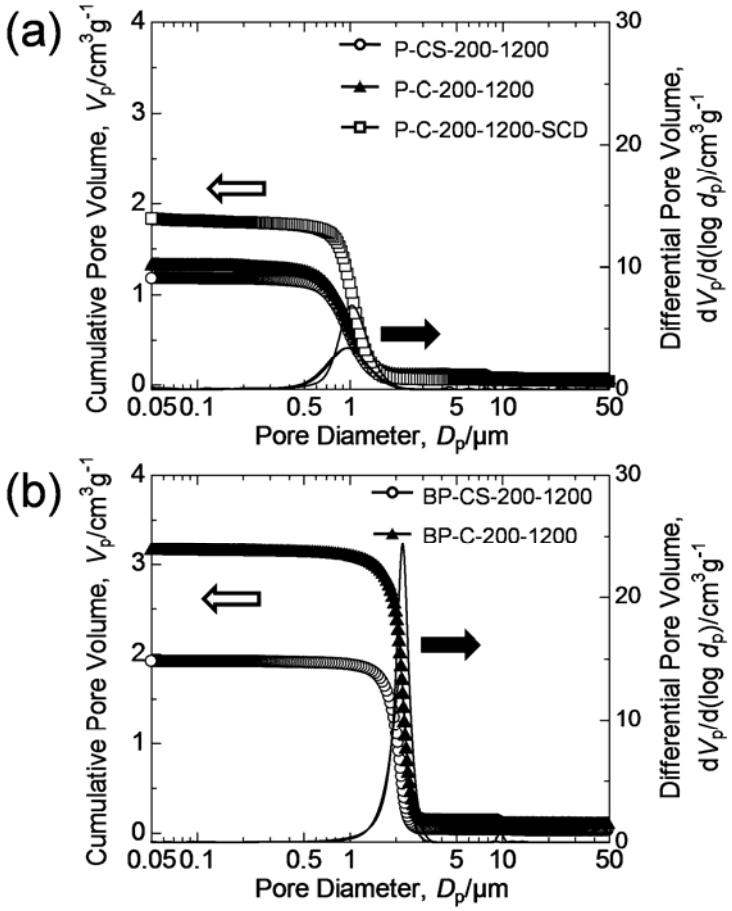

Figure 13